FUSE

Fungal Systematics and Evolution

VOLUME 8
DECEMBER 2021
PAGES 155–161

doi.org/10.3114/fuse.2021.08.12

Ophiostomatoid fungi including a new species associated with Asian larch bark beetle *Ips subelongatus*, in Heilongjiang (Northeast China)

R. Chang[1,2], M.J. Wingfield[1], S. Marincowitz[1], Z.W. de Beer[1], X. Zhou[1], T.A. Duong[1*]

[1]Department of Biochemistry, Genetics and Microbiology, Forestry and Agricultural Biotechnology Institute (FABI), University of Pretoria, Pretoria 0002, South Africa
[2]College of Life Sciences, Shandong Normal University, Jinan 250014, China

*Corresponding author: tuan.duong@fabi.up.ac.za

Key words:
Ophiostomatales
Microascales
new taxon
Scolytinae
vector

Abstract: *Ips subelongatus* (*Coleoptera*, *Scolytinae*) is an important bark beetle species that infests *Larix* spp. in Asia. Individuals of this beetle are vectors of ophiostomatoid fungi, on their exoskeletons, that are transmitted to infested trees. In this study, the symbiotic assemblage of ophiostomatoid fungi associated with *I. subelongatus* in Northeast China was studied. Fungal isolates were identified based on their morphological characters and sequences of ITS, beta-tubulin, elongation factor 1-alpha and calmodulin gene regions. In total, 48 isolates were collected and identified, residing in six taxa. These included a novel species, described here as *Ophiostoma gmelinii sp. nov.*

Citation: Chang R, Wingfield MJ, Marincowitz S, De Beer ZW, Zhou X, Duong TA (2021). Ophiostomatoid fungi including a new species associated with Asian larch bark beetle *Ips subelongatus*, in Heilongjiang (Northeast China). *Fungal Systematics and Evolution* **8**: 155–161. doi: 10.3114/fuse.2021.08.12
Received: 11 August 2021; **Accepted:** 8 November2021; **Effectively published online:** 18 November 2021
Corresponding editor: P.W. Crous

INTRODUCTION

The Asian larch bark beetle, *Ips subelongatus* (*Coleoptera*, *Scolytinae*), is the most important insect pest infesting various *Larix* (larch) species in China (Chen *et al.* 2015). This beetle is also found in other Eurasian countries including Japan, Mongolia, North Korea, Russia, and South Korea (Cognato 2015). *Ips subelongatus* typically infests weakened, wind-thrown, and fire-damaged trees, but it is also able to kill healthy trees when outbreaks result in substantial population growth (Zhang *et al.* 1992).

Ips subelongatus as well as other bark beetles and their associated phoretic mites are well-known vectors of ophiostomatalean and microascalean fungi (Six 2003, Hofstetter & Moser 2014). The best known genera are *Ophiostoma* and *Ceratocystis* respectively (De Beer & Wingfield 2013). Most of these fungi only cause discoloration of the sapwood of infested trees (Six 2003). However, some species such as the Dutch elm disease fungi (*Ophiostoma ulmi* and *O. novo-ulmi*) and species accommodated in *Ceratocystis sensu lato* are important tree pathogens (Brasier 2001, Roux & Wingfield 2009).

There have been several investigations considering the fungal associates of bark beetle *I. subelongatus* in China (Liu *et al.* 2017, Wang *et al.* 2020) and these have revealed 21 species. Specifically, the recent study by Wang *et al*. (2020) was the most extensive and included the description of eight new taxa. The present study arose from a collection of isolates made from the beetles and galleries of *I. subelongatus* infesting *Larix gmelinii* in Heilongjiang, China. Identification of these isolates based on DNA sequence comparisons showed that most were of known taxa. Three of isolates appeared to represent a novel taxon and the aim of this study was to test this hypothesis.

MATERIALS AND METHODS

Fungal collection

Samples for this study were collected in July 2011, during the flight season of *I. subelongatus,* from a natural forest in Heilongjiang (northeast China) where *L. gmelinii* was also present. A total of 44 beetles and 46 galleries were collected and used for fungal isolation. The isolation medium was 2 % malt extract agar [MEA: 20 g Difco agar, 20 g Difco Bacto™ malt extract (Becton, Dickinson & Company), 1 L deionized water] supplemented with 0.05 % streptomycin. Fungal spore drops were picked up directly from the galleries and inoculated onto MEA plates. Living beetles were placed onto the surface of MEA plates and let crawling for several minutes and removed thereafter. Dead beetles were crushed and spread onto MEA plates. The MEA plates were incubated at room temperature (~ 25 °C) until fungal growth was observed. Tips of hyphae were picked and transferred onto new MEA plates. All the isolates collected in this study have been maintained in Culture Collection (CMW) of the Forestry and Agricultural Biotechnology Institute (FABI), University of Pretoria, South Africa. Ex-type cultures of a new species were deposited in the culture collection (CBS) of the Westerdijk Fungal Biodiversity Institute, Utrecht, the Netherlands. Herbarium specimens established as dried cultures were deposited to South African National Collection of Fungi (PREM), Roodeplaat, Pretoria, South Africa.

DNA extraction and PCR

DNA was extracted from fresh mycelium grown on 2 % MEA following the instructions provided by PrepMan™ Ultra Sample Preparation Reagent (Applied Biosystems, Foster City, CA). The primers ITS1F and ITS4 (White *et al.* 1990; Gardes & Bruns 1993) were used to amplify the internal transcribed spacer region (ITS), the primers BT2a and BT2b (Glass & Donaldson 1995) were used to amplify the beta-tubulin (*BT*) gene, the primers EF2F (Marincowitz *et al.* 2015) and EF2R (Jacobs *et al.* 2004) were used to amplify the translation elongation factor 1-alpha gene (*EF*). The primers CL2F and CL2R (Duong *et al.* 2012) were used to amplify the calmodulin gene (*CAL*). PCR and sequencing were conducted using the methods described by Duong *et al.* (2012). All sequences were assembled and checked by forward and reverse sequence using Geneious v. 7.1.4 (Biomatters, Auckland, New Zealand).

DNA sequence analyses

The ITS sequences of all isolates were subjected to BLASTn searches against the NCBI GeneBank nucleotide database (http://blast.ncbi.nlm.nih.gov) for preliminary identification. Based on the BLAST results, datasets of *BT*, *EF* and *CAL* sequences for different genera and species complexes were compiled and analyzed separately. Sequence alignments were done using an online version of MAFFT v. 7.0 (Katoh & Standley 2013), and were further curated in MEGA v. 6 (Tamura *et al.* 2013). Maximum likelihood (ML) and Bayesian inference (BI) analyses were conducted using RAxML-HPC2 v. 8.2.4 (Stamatakis 2014) and MrBayes v. 3.2.6 (Ronquist *et al.* 2012) respectively; both are available from the CIPRES Science Gateway (Miller *et al.* 2010). For the BI analysis, trees were sampled every 100th generation for 5 M generations and 25 % of trees were discarded as burn-in phase. All alignments have been deposited in TreeBASE (https://treebase.org/) under the study number S28534.

Morphology and culture characteristics

Depending on the number of isolates available, two to three isolates per species were chosen for morphological examination. Fresh mycelium was inoculated onto MEA plates to which sterilized pine twigs (with bark) had been added to induce the production of sexual or asexual structures. Fungal structures were examined using a Nikon Eclipse Ni light microscope (Nikon, Japan) and a Nikon SMZ 18 dissection microscope attached with a Nikon DS-Ri2 camera. Up to 50 measurements were made for characteristic structures whenever available using the NIS Elements BR software. Measurements are presented as "maximum – minimum" except for spores where "average ± standard deviation" was additionally presented.

Growth rates were determined at seven temperatures ranging from 5 to 35 °C at 5 °C intervals. Mycelial plugs (5 mm diam) were transferred from the margins of actively growing cultures to the centers of 90 mm Petri dishes containing 2 % MEA. Two diameter measurements perpendicular to each other were made of the colonies and the daily growth rate was calculated.

RESULTS

A total of 48 ophiostomatoid isolates were obtained. Twenty-one were obtained from the galleries of the beetle and the remaining isolates were from the beetles themselves. BLAST searches of the ITS sequences showed that the isolates collected in this study resided in three genera, *Endoconidiophora*, *Ophiostoma*, and *Sporothrix* (Table 1). Analyses of ITS (Fig. 1), *BT*, *EF* and *CAL* sequences suggested that these isolates resided in six taxa, five of which were known species *i.e.*, *O. hongxingense* (11 isolates) (Fig. S1), *O. peniculi* (two isolates) (Fig. S1), *O. pseudobicolor* (one isolate) (Fig. S2), *Sporothrix cf. abietina* (two isolates) (Fig. S3), and *Endoconidiophora fujiensis* (five isolates) (Fig. S4), and three isolates belonging to a novel species (Fig. 2) which is described below.

Taxonomy

Ophiostoma gmelinii R.L. Chang, Z.W. de Beer & M.J. Wingf., ***sp. nov.*** MycoBank MB 840569. Fig. 3.

Etymology: The epithet *gmelinii* refers to *Larix gmelinii,* a tree that *Ips subelongatus* infests in China.

Diagnosis: Ophiostoma gmelinii differed from its closest phylogenetic relatives, *O. rufum* and *O. xinganense*, in the size of conidia, growth rate, and lack of pesotum-like asexual morph.

Sexual morph not observed. *Asexual morph* sporothrix-like. *Mycelium* mostly submerged, densely compacted, hyaline, sometimes developing brown strings of hyphae with age. *Conidiophores* simple, upright, flexuous, rarely branched, septate, occasionally reduced to conidiogenous cells, 4–290 × 1–2 µm (4–30 µm long when reduced to conidiogenous cells). *Conidiogenous cells* blastic, denticulate, often showing sympodial growth, terminal, sometimes directly borne on vegetative hyphae. *Conidia* hyaline, mostly oblong, aseptate, the apex often slightly inflated, tapering abruptly to the pointed base, 4.5–8 × 2–3 µm (6.4 ± 0.96 × 2 ± 0.22 µm).

Culture characteristics: Colony shiny, smooth, colorless to whitish, developing pigmented zone or patches of hyphal strings when aged or damaged. Optimum growth at 25 °C (2.8 mm / d), followed by 20 °C (2.3 mm / d), 15 °C (1.7 mm / d), 10 °C (1 mm / d), 30 °C (0.9 mm / d), no growth at 5 and 35 °C.

Typus: **China**, Heilongjiang province, from gallery of *Ips subelongatus* on *Larix gmelinii*, 2011, coll. *X.D. Zhou* (**holotype** PREM 61562, culture ex-type CMW 40463 = CBS 141909).

Additional material examined: **China**, Heilongjiang province, from gallery of *Ips subelongatus* on *Larix gmelinii*, 2011, coll. *X.D. Zhou,* PREM 61564, culture CMW 40464 = CBS 141911.

Notes: The newly described *O. gmelinii* resides in the *O. piceae* species complex. Based on the analyses of *BT* sequences, all the isolates of this species formed a single clade together with *O. rufum,* which was recently described from the Czech Republic (Jankowiak *et al.* 2019), and *O. xinganense* described from China (Wang *et al.* 2020). This clade had a strong bootstrap support in the ML analysis but not in the case of the BI analysis (Fig. 2). However, based on the analyses of ITS sequences, *O. gmelinii* formed a well-resolved clade and this formed a sister clade with *O. genhense* and *O. multisynnematum*. *Ophiostoma rufum* grouped with *O. piceae*, *O. micans*, and other species. In the *EF* tree, all isolates of *O. gmelinii* formed a sister clade with *O.*

Table 1. Isolates of ophiostomatoid fungi obtained from *I. subelongatus* on *Larix gmelinii* in Heilongjiang and used in phylogenetic analyses.

	Isolate number[1,2]			GenBank number[4]			
Species	**CMW**	**CBS**	**B/G[3]**	**ITS**	***BT***	***EF***	***CAL***
Endoconidiophora	40450		B	MW581513	MW579724	MW579746	n/a
fujiensis	40453		B	MW581514	MW579725	MW579747	n/a
	40460		B	MW581515	MW579726	MW579748	n/a
	40465		G	MW581516	MW579727	MW579749	n/a
	40479		B	MW581517	MW579728	MW579750	n/a
Ophiostoma gmelinii sp. nov.	40447		B	MW581494	MW579705	MW579729	n/a
	40463 H	141909	B	MW581495	MW579706	MW579730	n/a
	40464	141911	B	MW581496	MW579707	MW579731	n/a
O. hongxingense	40448		G	MW581498	MW579709	MW579733	n/a
	40455		G	MW581499	MW579710	MW579734	n/a
	40466		B	MW581500	MW579711	MW579735	n/a
	40467		B	MW581501	MW579712	MW579736	n/a
	40469		B	MW581502	MW579713	MW579737	n/a
	40474		B	MW581503	MW579714	MW579738	n/a
	40477		B	MW581504	MW579715	MW579739	n/a
	40483		B	MW581505	MW579716	MW579740	n/a
	40485		B	MW581506	MW579717	n/a	n/a
	40486		B	MW581507	MW579718	MW579741	n/a
	40487		B	MW581508	MW579719	MW579742	n/a
O. peniculi	40444		G	MW581509	MW579720	MW579743	n/a
	40472		B	MW581510	MW579721	MW579744	n/a
O. pseudobicolor	40478		B	MW581497	MW579708	MW579732	n/a
Sporothrix cf. abietina	40475		B	MW581511	MW579722	n/a	MW579751
	40454		G	MW581512	MW579723	MW579745	MW579752

[1] CMW: Culture Collection of the Forestry and Agricultural Biotechnology Institute (FABI), University of Pretoria, Pretoria, South Africa; CBS: Culture Collection of the Westerdijk Fungal Biodiversity Institute, Utrecht, the Netherlands.

[2] H = ex-holotype isolate.

[3] B = beetle; G = gallery.

[4] ITS = internal transcribed spacer regions 1 and 2 of the nuclear ribosomal DNA operon, including the 5.8S region; *BT* = beta-tubulin; *EF* = translation elongation factor 1-alpha; *CAL* = calmodulin.

flexuosum, O. multisynnematum and *O. genhense*. Collectively, these analyses resolved *O. gmelinii* as a distinct species in the *O. piceae* species complex as defined by Yin *et al*. (2016).

Morphological characters of *O. gmelinii* differed from its closest relatives *O. rufum* and *O. xinganense*. The conidia of *O. gmelinii* were larger than those of *O. rufum* (Jankowiak *et al.* 2019) but similar to those of *O. xinganense* (Wang *et al.* 2020). The growth rate of *O. gmelinii* was faster than in *O. rufum,* but much slower than in *O. xinganense*. In addition, *O. gmelinii* and *O. xinganense* are able to grow, albeit slowly at 30 °C, but *O. rufum* is not able to grow at this temperature (Jankowiak *et al.* 2019). Only a sporothrix-like asexual state was found in *O. gmelinii*, which is different to most of the other species in the *O. piceae* complex. These fungi typically produce pesotum-like synnemata as well as a sporothrix-like asexual morph (Yin *et al.* 2016, Wang *et al*. 2020). All the species in this complex, including the newly described *O. gmelinii*, are from conifer hosts (Yin *et al.* 2016, Jankowiak *et al*. 2019).

DISCUSSION

In this study, 48 isolates of ophiostomatoid fungi were obtained from beetles of *I. subelongatus* or its galleries. Six taxa were identified, residing in either the *Microascales* (one species) or the *Ophiostomatales*, including one new species. All the known species had previously been reported from China. *Sporothrix cf. abietina* was isolated from *I. subelongatus* for the first time.

Previous studies have revealed 21 species associated with *I. subelongatus* in China with 14 were new to science (Paciura *et al*. 2010, Wang *et al.* 2016, Liu *et al*. 2017, Wang *et al.* 2020). The present study adds two more species to this list. These results suggest that the fungal symbionts of *I. subelongatus* have now been relatively well sampled. As is true for many other ophiostomatoid fungi associated with conifer-infesting bark beetles, relatively little is known regarding their biology. In this regard, most are thought not to play a role in killing trees (Six & Wingfield, 2011). Although in the case of *Endoconidiophora fujiensis* (Yamaoka *et al.* 1998), which is a sister species to the *E. laricicola* associate of

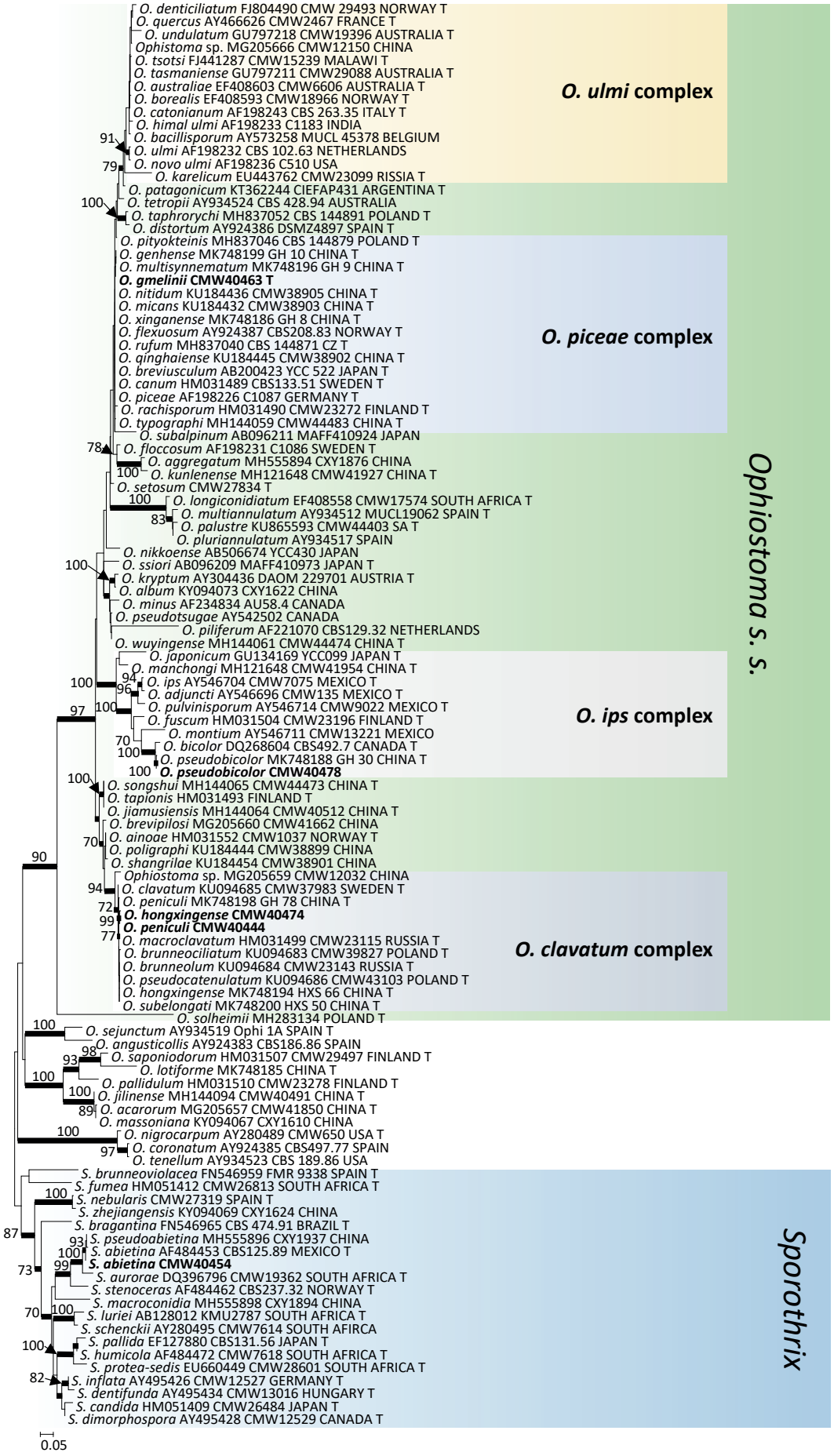

Fig. 1. Phylogram obtained from ML analyses of the ITS region of *Ophiostoma* and *Sporothrix*. Sequences obtained in this study are printed in bold type. Maximum-likelihood bootstrap support values (1 000 replicates) above 70 % are indicated at the nodes. Bayesian inference posterior probabilities (above 0.9) are indicated by bold lines at the relevant branches. T = ex-type cultures.

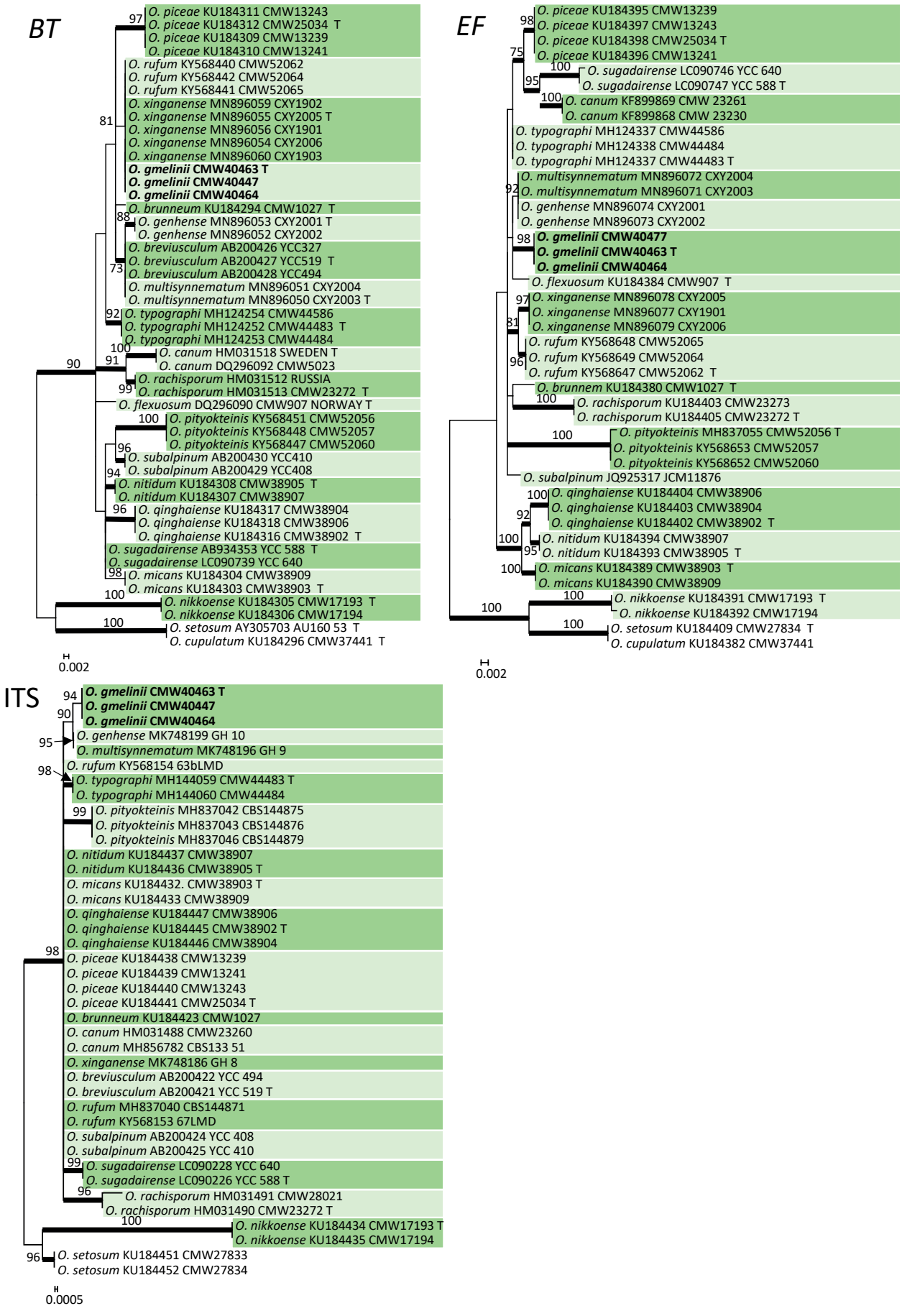

Fig. 2. Phylogrammes obtained from ML analyses of the ITS region, and the partial *BT* and *EF* gene regions of the *O. piceae* species complex. Isolates of the novel species are printed in bold type. Maximum-likelihood bootstrap support values (1 000 replicates) above 70 % are indicated at the nodes. Bayesian inference posterior probabilities (above 0.9) are indicated by bold lines at the relevant branches. T = ex-type cultures.

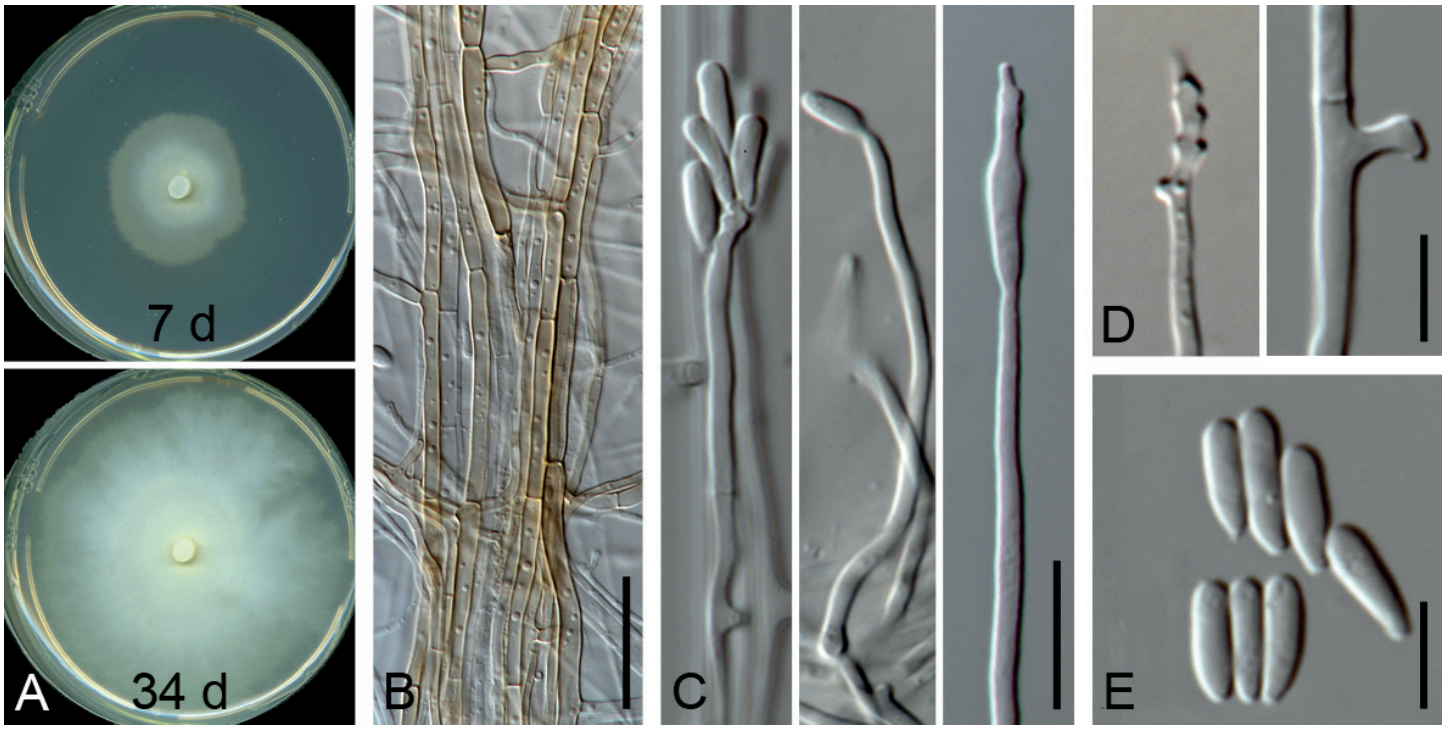

Fig. 3. Microscopic features of *Ophiostoma gmelinii sp. nov.* (ex-holotype, CMW 40463 = CBS 141909). **A.** Colony grown at 25 °C for 7 and 34 d in the dark. **B.** String of pigmented hyphae found in aged culture. **C.** Conidiophore. **D.** Conidiogenous cell. **E.** Conidia. Scale bars: B = 25 µm; C, D = 10 µm; E = 5 µm.

Ips cembrae (Marin *et al.* 2005) and the *E. polonica* associate of *I. typographus* (Krokene & Solheim, 1998), this question remains contentious (Lieutier *et al.* 2009, Biedermann *et al.* 2019)

Ips subelongatus has a wide distribution in China (Yang *et al.* 2007), including Heilongjiang, Jilin, Liaoning, Xinjiang, Gansu, Shandong, Shanxi, Hebei, Beijing, Zhejiang and Yunnan provinces and in other parts of Asia (Cognato 2015). All the studies on the fungal associates of this beetle in China have been in the north eastern parts of this country. It would thus be valuable in future studies to compare the fungal associates of this insect in different parts of China, as well as in other areas of East Asia.

ACKNOWLEDGEMENTS

We thank members of Tree Protection and Cooperation Programme (TPCP), the Department of Science and Technology (DST)-National Research Foundations (NRF), Center of Excellence in Plant Health Biotechnology (CPHB), and University of Pretoria, Pretoria, South Africa for financial support.

Conflict of interest: The authors declare that there is no conflict of interest.

REFERENCES

Biedermann PHW, Müller J, Grégoire J-C, *et al.* (2019). Bark beetle population dynamics in the Anthropocene: challenges and solutions. *Trends in Ecology & Evolution* **34**: 914–924.

Brasier CM (2001). Rapid evolution of introduced plant pathogens via interspecific hybridization: hybridization is leading to rapid evolution of Dutch elm disease and other fungal plant pathogens. *BioScience* **51**: 123–133.

Chen DF, Li YJ, Zhang QH, *et al.* (2015). Population divergence of aggregation pheromone responses in *Ips subelongatus* in northeastern China. *Insect Science* **23**: 728–738.

Cognato AI (2015). Biology, systematics, and evolution of *Ips*. In: *Bark Beetles: Biology and ecology of native and invasive species* (Vega FE, Hofstetter RW, eds). Academic Press, San Diego: 351–370.

De Beer ZW, Wingfield MJ (2013). Emerging lineages in the *Ophiostomatales*. In: *The Ophiostomatoid Fungi: Expanding Frontiers* (Seifert KA, De Beer ZW, Wingfield MJ, eds). CBS, Utrecht, The Netherlands: 21–46.

Duong TA, De Beer ZW, Wingfield BD, *et al.* (2012). Phylogeny and taxonomy of species in the *Grosmannia serpens* complex. *Mycologia* **104**: 715–732.

Gardes M, Bruns TD (1993). ITS primers with enhanced specificity for basidiomycetes-application to the identification of mycorrhizae and rusts. *Molecular Ecology* **2**: 113–118.

Glass NL, Donaldson GC (1995). Development of primer sets designed for use with the PCR to amplify conserved genes from filamentous Ascomycetes. *Applied and Environmental Microbiology* **61**: 1323–1330.

Hofstetter RW, Moser JC (2014). The role of mites in insect-fungus associations. *Annual Review of Entomology* **59**: 537–557.

Jacobs K, Bergdahl DR, Wingfield MJ, *et al.* (2004). *Leptographium wingfieldii* introduced into North America and found associated with exotic *Tomicus piniperda* and native bark beetles. *Mycological Research* **108**: 411–418.

Jankowiak R, Bilański P, Strzałka B, *et al.* (2019). Four new *Ophiostoma* species associated with conifer- and hardwood-infesting bark and ambrosia beetles from the Czech Republic and Poland. *Antonie van Leeuwenhoek* **112**: 1501–1521.

Katoh K, Standley DM (2013). MAFFT multiple sequence alignment software version 7: improvements in performance and usability. *Molecular Biology and Evolution* **30**: 772–780.

Krokene P, Solheim H (1998). Pathogenicity of four blue-stain fungi

associated with aggressive and non aggressive bark beetles. *Phytopathology* **88**: 39–44.

Lieutier F, Yart A, Salle A (2009). Stimulation of tree defenses by ophiostomatoid fungi can explain attack success of bark beetles on conifers. *Annals of Forest Science* **66**: 801.

Liu XW, Wang HM, Lü Q, *et al.* (2017). Taxonomy and pathogenicity of *Leptographium* species associated with *Ips subelongatus* infestations of *Larix* spp. in northern China, including two new species. *Mycological Progress* **16**: 1–13.

Marin M, Preisig O, Wingfield BD, *et al.* (2005). Phenotypic and DNA sequence data comparisons reveal three discrete species in the *Ceratocystis polonica* species complex. *Mycological Research* **109**: 1137–1148.

Marincowitz S, Duong TA, De Beer ZW, *et al.* (2015). *Cornuvesica*: A little known mycophilic genus with a unique biology and unexpected new species. *Fungal Biology* **119**: 615–630.

Miller MA, Pfeiffer W, Schwartz T (2010). Creating the CIPRES Science Gateway for inference of large phylogenetic trees. Institute of Electrical and Electronics Engineers, New Orleans, LA: 1–8.

Paciura D, De Beer ZW, Jacobs K, *et al.* (2010). Eight new *Leptographium* species associated with tree-infesting bark beetles in China. *Persoonia* **25**: 94–108.

Ronquist F, Teslenko M, van der Mark P, *et al*. (2012) MrBayes 3.2: efficient Bayesian phylogenetic inference and model choice across a large model space. *Systematic Biology* **61**: 539–542.

Roux J, Wingfield MJ (2009). *Ceratocystis* species: emerging pathogens of non-native plantation *Eucalyptus* and *Acacia* species. *South Forests* **71**: 115–120.

Six DL (2003). Bark beetle-fungus symbioses. In: *Insect Symbiosis* (Bourtzis K, Miller T, eds), CRC Press, Boca Raton, Florida USA: 77–114.

Six DL, Wingfield MJ (2011). The role of phytopathogenicity in bark beetle-fungus symbioses: a challenge to the classic paradigm. *Annual Review of Entomology* **56**: 255–272.

Stamatakis A (2014) RAxML version 8: a tool for phylogenetic analysis and post-analysis of large phylogenies. *Bioinformatics* **30**: 1312–1313.

Tamura K, Stecher G, Peterson D, *et al.* (2013). MEGA6: molecular evolutionary genetics analysis version 6.0. *Molecular Biology and Evolution* **30**: 2725–2729.

Wang H, Lu Q, Meng X, *et al.* (2016). *Ophiostoma olgensis*, a new species associated with *Larix* spp . and *Ips subelongatus* in northern China. *Phytotaxa* **282**: 282–290.

Wang Z, Liu Y, Wang H, *et al.* (2020). Ophiostomatoid fungi associated with *Ips subelongatus*, including eight new species from northeastern China. *IMA Fungus* **11**: 3.

White TJ, Bruns T, Lee S, *et al.* (1990). Amplification and direct sequencing of fungal ribosomal RNA genes for phylogenetics. In: *PCR protocols: a guide to methods and applications* (Innis MA, Gelfand DH, Sninsky JJ, White TJ, eds). Academic Press, San Diego (California): 315–322.

Yamaoka Y, Wingfield M, Ohsawa M, *et al.* (1998). Ophiostomatoid fungi associated with *Ips cembrae* in Japan and their pathogenicity of Japanese larch. *Mycoscience* **39**: 367–378.

Yang J, Lin Q, Chen G (2007). Risk analysis of *Ips subelongatus* motschulsky (in Chinese). *Journal of Northeast Forestry University* **35**: 60–63.

Yin ML, Wingfield MJ, Zhou XD, *et al.* (2016). Multigene phylogenies and morphological characterization of five new *Ophiostoma* spp. associated with spruce-infesting bark beetles in China. *Fungal Biology* **120**: 454–470.

Zhang QH, Byers JA, Schlyter F (1992). Optimal attack density in the larch bark beetle, *Ips cembrae* (*Coleoptera*: *Scolytidae*). *Journal of Applied Ecology* **29**: 672–678.

Supplementary Material: http://fuse-journal.org/

Fig. S1. Phylogram obtained from ML analyses of the partial *BT* and *EF* gene sequences of the *O. clavatum* species complex. Sequences obtained in this study are printed in bold type. Maximum-likelihood bootstrap support values (1 000 replicates) above 70 % are indicated at the nodes. Bayesian inference posterior probabilities (above 0.9) are indicated by bold lines at the relevant branches. T = ex-type cultures.

Fig. S2. Phylogram obtained from ML analyses of the ITS region and the partial *BT* gene of the *O. ips* species complex. Sequences obtained in this study are printed in bold type. Maximum-likelihood bootstrap support values (1 000 replicates) above 70 % are indicated at the nodes. The Bayesian inference posterior probabilities (above 0.9) are indicated by bold lines at the relevant branches. T = ex-type cultures.

Fig. S3. Phylogram obtained from ML analyses of the ITS region, and the partial *BT* and *CAL* gene sequences of the *Sporothrix gossypina* species complex. Sequences obtained in this study are printed in bold type. Maximum-likelihood bootstrap support values (1 000 replicates) above 70 % are indicated at the nodes. Bayesian inference posterior probabilities (above 0.9) are indicated by bold lines at the relevant branches. T = ex-type cultures.

Fig. S4. Phylogram obtained from ML analyses of the ITS region, and the partial *BT* and *EF* gene sequences of *Endoconidiophra*. Sequences obtained in this study are printed in bold type. Maximum-likelihood bootstrap support values (1 000 replicates) above 70 % are indicated at the nodes. Bayesian inference posterior probabilities (above 0.9) are indicated by bold lines at the relevant branches. T = ex-type cultures.

Fig. S1

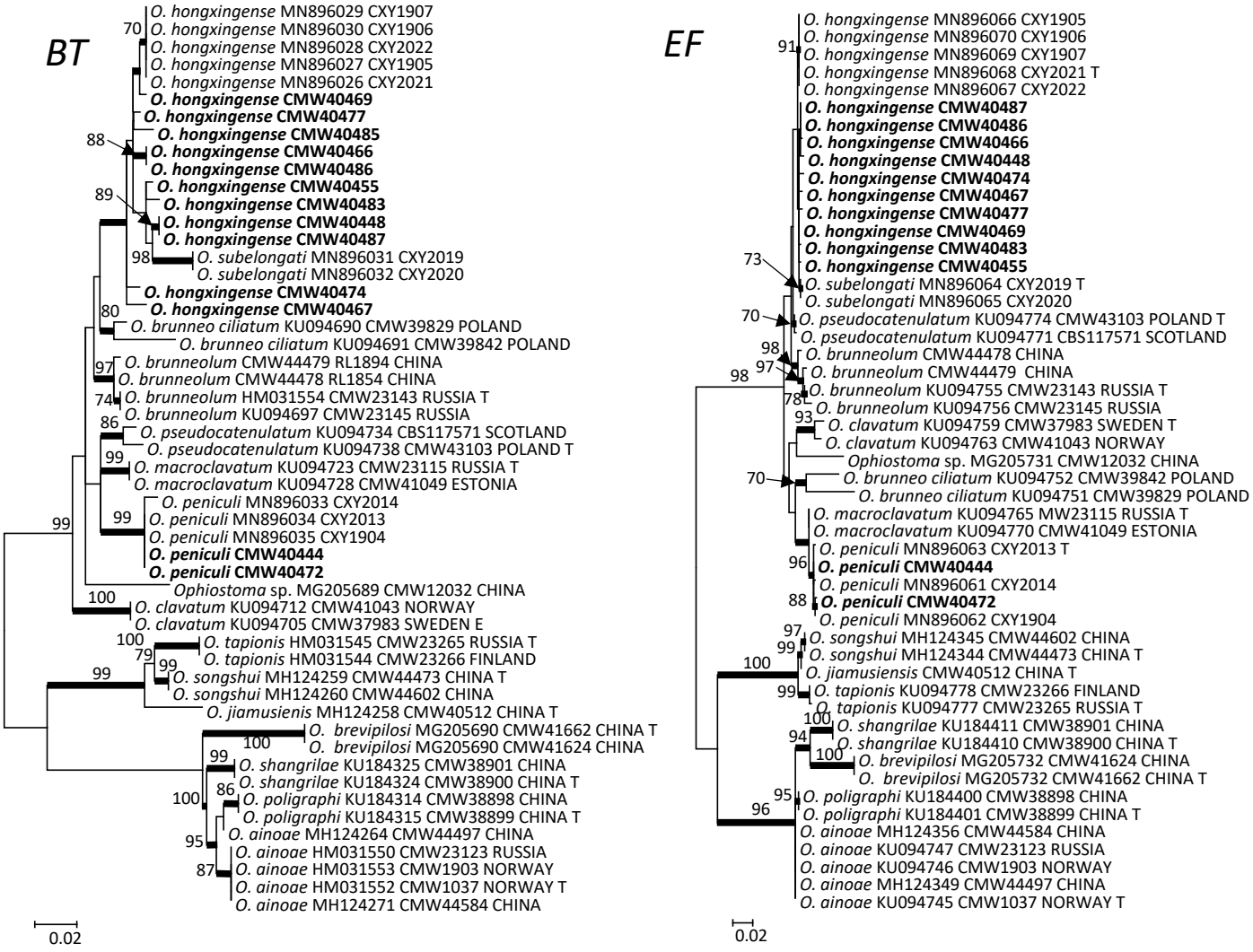

Fig. S1. Phylogram obtained from ML analyses of the partial *BT* and *EF* gene sequences of the *O. clavatum* species complex. Sequences obtained in this study are printed in bold type. Maximum-likelihood bootstrap support values (1 000 replicates) above 70 % are indicated at the nodes. Bayesian inference posterior probabilities (above 0.9) are indicated by bold lines at the relevant branches. T = ex-type cultures.

Fig. S2

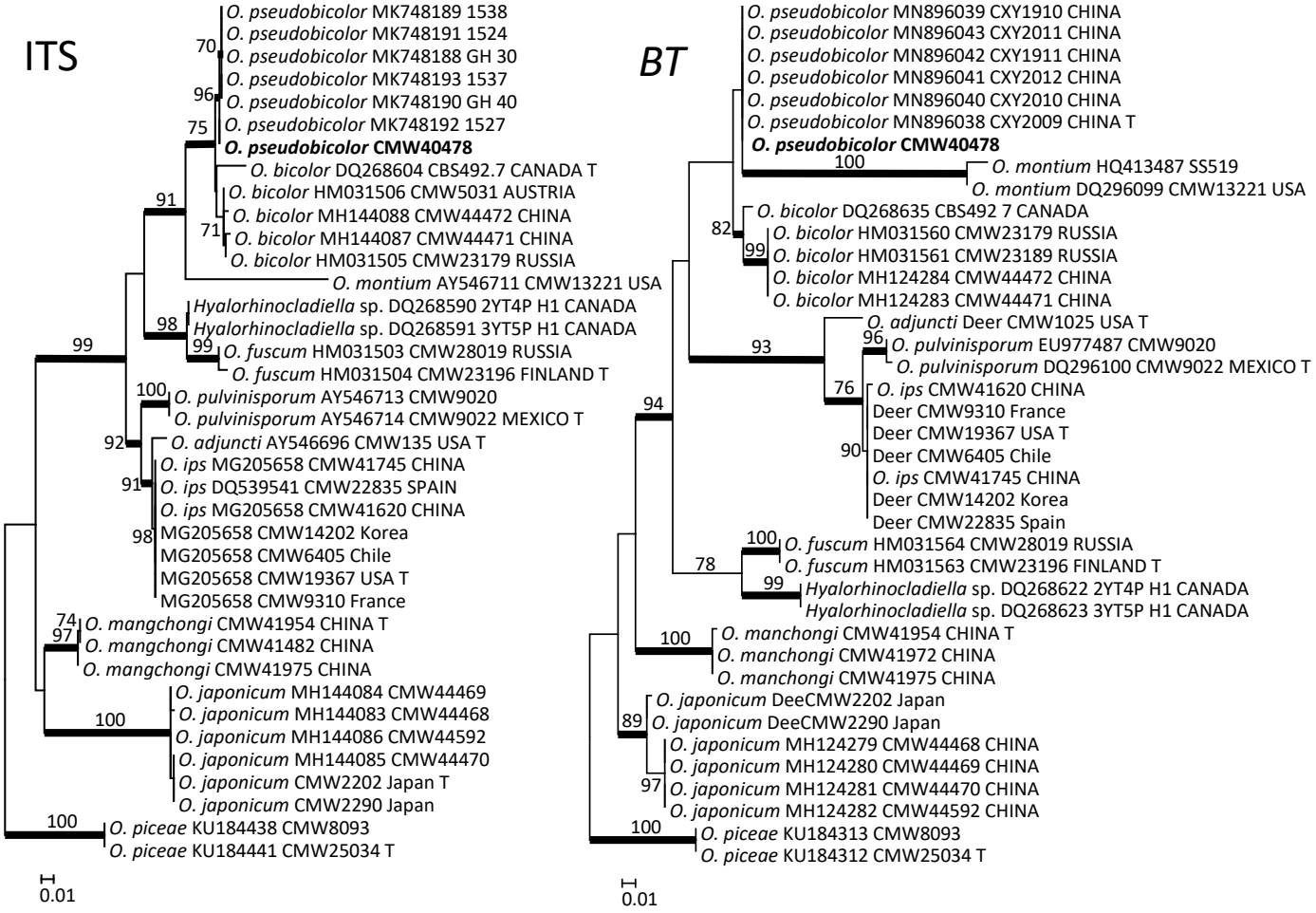

Fig. S2. Phylogram obtained from ML analyses of the ITS region and the partial *BT* gene of the *O. ips* species complex. Sequences obtained in this study are printed in bold type. Maximum-likelihood bootstrap support values (1 000 replicates) above 70 % are indicated at the nodes. The Bayesian inference posterior probabilities (above 0.9) are indicated by bold lines at the relevant branches. T = ex-type cultures.

Fig. S3

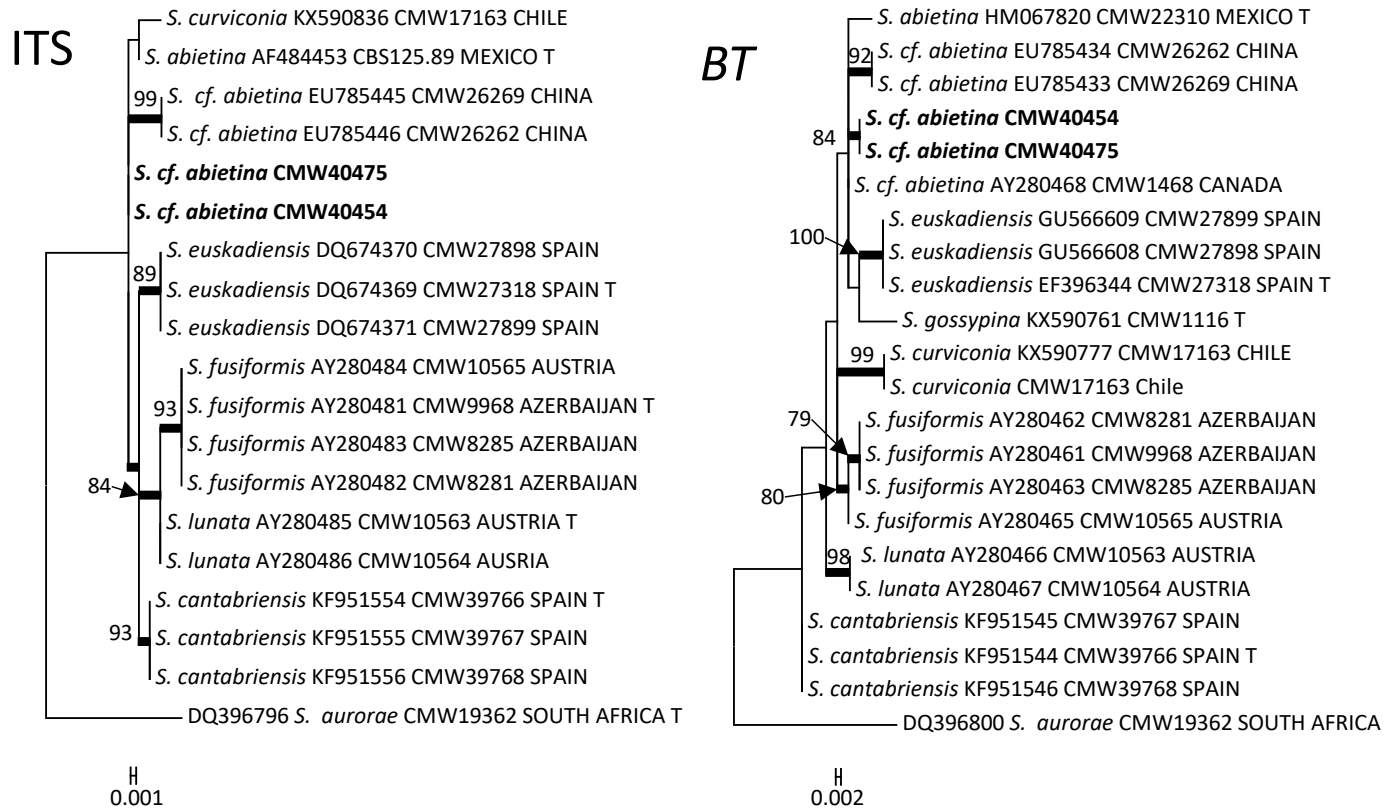

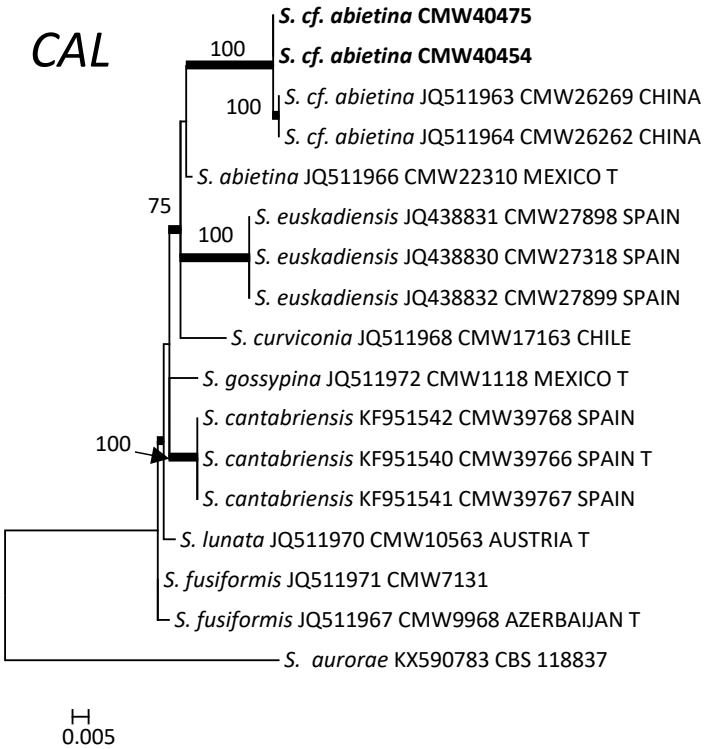

Fig. S3. Phylogram obtained from ML analyses of the ITS region, and the partial *BT* and *CAL* gene sequences of the *Sporothrix gossypina* species complex. Sequences obtained in this study are printed in bold type. Maximum-likelihood bootstrap support values (1 000 replicates) above 70 % are indicated at the nodes. Bayesian inference posterior probabilities (above 0.9) are indicated by bold lines at the relevant branches. T = ex-type cultures.

Fig. S4

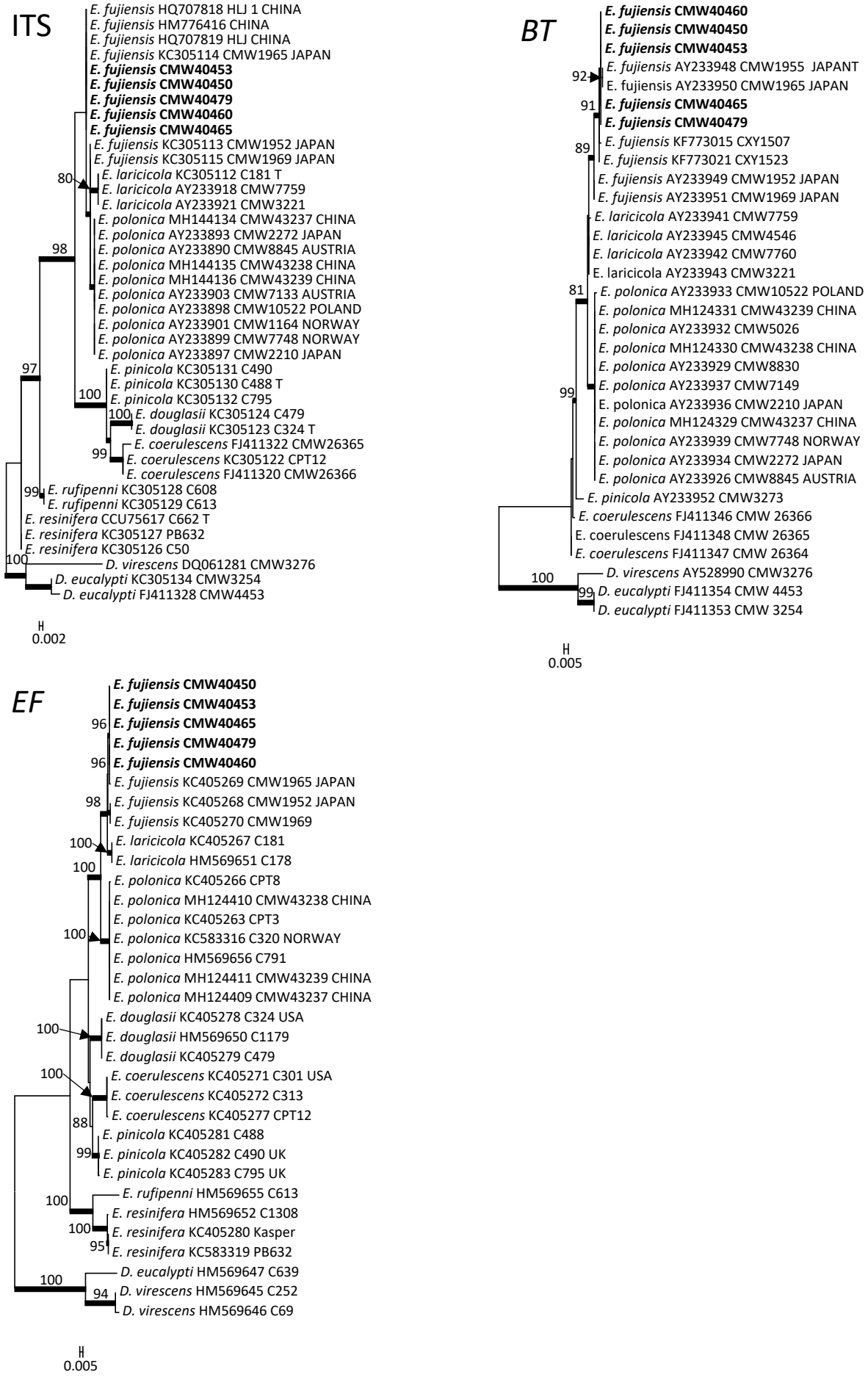

Fig. S4. Phylogram obtained from ML analyses of the ITS region, and the partial *BT* and *EF* gene sequences of *Endoconidiophra*. Sequences obtained in this study are printed in bold type. Maximum-likelihood bootstrap support values (1 000 replicates) above 70 % are indicated at the nodes. Bayesian inference posterior probabilities (above 0.9) are indicated by bold lines at the relevant branches. T = ex-type cultures.